Sensors and Materials, Vol. 35, No. 8 (2023) 2755–2770
MYU Tokyo

S & M 3352

Fixed-time Stabilized Adaptive Sliding Mode Control for Synchronizations of Neuro-cell Circuit Systems

Chuanjian Liang, Chi-Hsin Yang,* Ruizhao Yang,
Kun-Chieh Wang, and Hong-Yi Chen

School of Physics and Telecommunication Engineering, Yulin Normal University,
Yulin City, Guangxi 53700, China

(Received April 7, 2023; accepted July 5, 2023)

Keywords: integral-type, sliding mode, fixed-time stabilized, synchronizations, neuro-cell circuit system, voltage-sensing equipment

We propose an adaptive integral-type fixed-time stabilized sliding mode (IFSSM) control approach to simultaneously solve the control problems of state synchronization and anti-synchronization between two space-clamp FitzHugh–Nagumo (SFHN) neuro-cell circuit systems or neuronal circuits. The novel IFSSM consists of the fractional-powered, proportional, and integral terms of two state variables. The special characteristic of the IFSSM is that, on a sliding surface, one of the state variables becomes stable at a fixed time, then the other state variable is exponentially stabilized in sequence. Furthermore, two theorems related to the stability are provided and proven to demonstrate that the designed control approach can achieve the control goal. Numerical simulations are carried out to verify the validity of the proposed control approach for future practical realization in neuronal circuits. The developed control schemes can be implemented by the hardware circuit realization with voltage-sensing equipment.

1. Introduction

The architecture of circuits implemented for neuronal systems has recently been explored.(1) The frontier viewpoint is that the different types of neuronal circuit are the elementary components of an artificial neuro-cell network system, highlighting the importance of developing neuronal circuits based on the behavior of a neuro-cell. The establishment of neuronal circuits can accelerate the application of themes in artificial intelligence. Basically, an artificial neuro-cell network system requires the ability to rapidly adapt to unpredictable environments. This requirement has motivated the use of machine learning technologies to solve the difficult and complex problems of such systems.(2)

To study the behavior of a neuro-cell, various biomathematical models such as the Hodgkin–Huxley (HH),(3) Hindmarsh–Rose,(4) and FitzHugh–Nagumo (FHN)(5–7) neuron models have been proposed. The HH neuron model is a relatively complete mathematical model and consists of a set of fourth-order nonlinear differential equations that describe the dynamics of the voltage

*Corresponding author: e-mail: yang2020@ylu.edu.cn
https://doi.org/10.18494/SAM4452

ISSN 0914-4935

of the neuron membrane base using the principles of electrochemistry. However, it contains four state variables and many system parameters, increasing the difficulty of its application. To simplify the analysis of the neuro-cell system, the traditional space-clamped FitzHugh–Nagumo (SFHN) neuron model[7] is more convenient for investigating the dynamic behavior of a neuro-cell system. Previous studies on the chaos and bifurcation of the SFHN neuron model are reviewed in Refs. 8 and 9.

To extend the practical application of the traditional SFHN neuron model, circuits are implemented using various technologies, such as analogical electronic circuits,[10–12] feedback circuits consisting of operational amplifiers and resistors,[13] very large scale integration (VLSI),[14] field-programmable gate arrays (FPGAs),[15] and field-effect transistors (FETs).[16] Moreover, in the framework of the traditional SFHN neuro-cell system, many new types of neuronal circuit system have been proposed, such as thermosensitive neuron,[17] piezoelectric neuron,[18] photosensitive neuron,[19,20] and neuronal circuit systems with electromagnetic induction.[21–23] Such new types of neuronal circuit are contributing to the development of multidiscipline applications in science and technology. The various types of neuronal circuit are helpful for realizing novel and more practical neuronal circuit control systems. It is therefore of practical significance to study new control schemes of neural cell circuit systems.

Because the HH neuron model[3] is difficult to apply, the alternative SFHN neuro-cell model, which has two state variables, was developed. The dynamical system adopts the nonlinear circuit reported in Ref. 20 for analogical simulation, as shown in Fig. 1. The through current $iL(t)$ of the induction coil L and the cross voltage $v(t)$ of the nonlinear resistor NR are the state variables of the system. C, L, R, and RS are the system parameters and $VS(t)$ is the input excitation.

For brevity of this paper, the derivation of the nondimensional dynamical system is omitted (see Ref. 20 for details). The state variables of an SFHN neuron are analogized by the corresponding voltages in the circuits. Therefore, the time responses of an electrical SFHN neuronal circuit for feedback control can be sensed by applying voltage-sensing equipment. Furthermore, the control schemes developed for synchronization are realized by applying a hardware circuit with sensing equipment.[24]

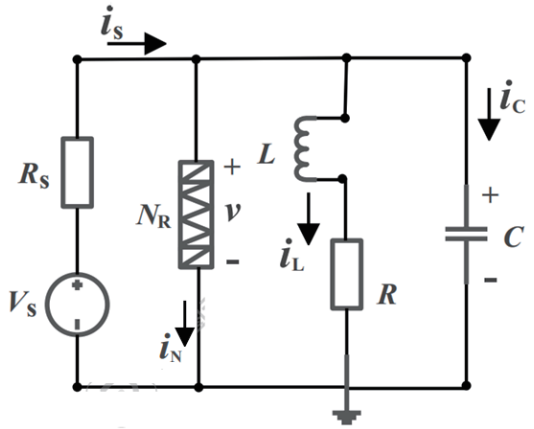

Fig. 1. Circuit implementation of the SFHN neuro-cell model.

The SFHN neuro-cell model can be represented by nonlinear non-autonomous differential equations with respect to the normalized time t:[8]

$$\begin{cases} \dot{x}_1 = -x_1(x_1-1)(x_1-\alpha) - y_1 + I_{\text{ion\_}m} + I_m \cos(\omega_m t) + \delta(t) + \Delta(x_1, y_1) \\ \dot{y}_1 = \beta(\gamma x_1 - y_1) \end{cases}. \quad (1)$$

The variable x_1 is a fast state, which models the membrane potential of the neuron cell. The variable y_1 is a slow state, which represents the recovery of the membrane potential. The system parameters α, β, and γ govern the dynamics of the neuro-cell model. The system uncertainty $\Delta(x_1, y_1)$ and the external disturbance $\delta(t)$ are assumed to be bounded and to satisfy

$$0 \le \left|\Delta(x_1, y_1)\right| \le D_1 \quad , \quad 0 \le \left|\delta(t)\right| \le D_2 . \quad (2)$$

I_{ion_m} in Eq. (1) represents the ionic current inside the master neuro-cell and $I_m\cos(\omega_1 t)$ represents external electrical stimulation (EES) with amplitude I_m and frequency $f_m = \omega_m/2\pi$. As shown in Fig. 2, the SFHN neuron cell exhibits chaotic dynamics for the parameter value set[8] $\alpha = 0.25$, $\beta = 0.02$, and $\gamma = 0.25$, $I_{ion\_m} = 0.082$, $I_m = 0.055$, $\omega_m = 0.1$ with the initial conditions $(x_1(0), y_1(0))=(0.2, 0.16)$.

In previous studies on control problems for SFHN neuron models, chaotic control in an SFHN neuron model by an adaptive passive control method was addressed.[8] State synchronization between two SFHN neurons subjected to EES by applying different schemes such as back-stepping control,[25] adaptive control,[26] and linear matrix inequality (LMI)-based adaptive control technologies was introduced.[27] By considering different EESs and ionic currents between two SFHN neurons, state synchronization was achieved in Ref. 28, in which robust adaptive sliding mode control (SMC) was proposed, and in Ref. 29, in which SMC with an

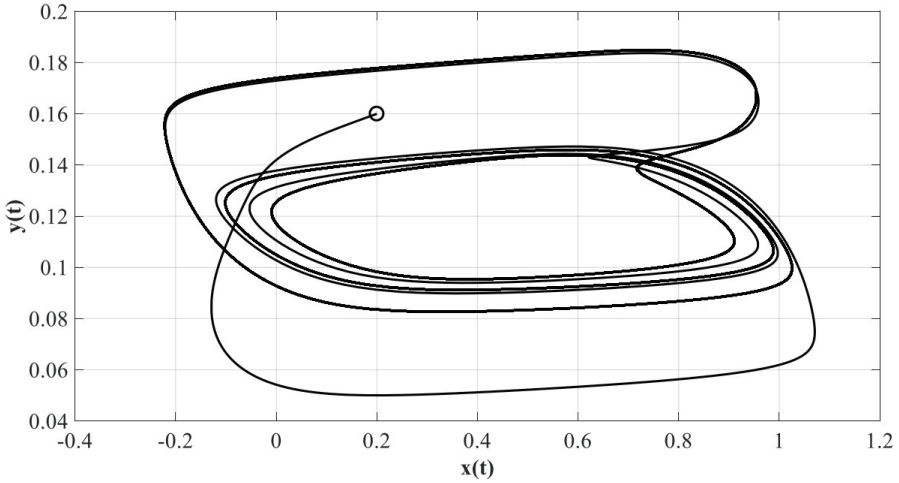

Fig. 2. State trajectory of the SFHN neuro-cell circuit system.

input–output linearized approach was developed. For coupled FHN neuron networks, synchronizations were achieved by employing a typical robust SMC scheme,[30] by adaptive time-delay feedback control,[31] or by lag synchronization using a feedback control scheme.[32] For the new types of FHN neuron system, the finite-time synchronization of a dual-memristor-based network has been introduced.[33] State- and phase-coupling synchronizations were developed for photosensitive FHN neurons in Refs. 34 and 35.

The motivation of this study emerged from the following observations. To achieve state synchronization between two SFHN neuro-cell systems, the main idea of the SMCs reported in past studies is to follow the error state trajectory to arrive at and remain on the sliding surface in the phase plane, which in Ref. 28 was a line with a negative slope and in Ref. 36 was a curve. Then, the error states were simultaneously converged to the origin along the defined sliding surface. The mathematical model of the SFHN neuro-cell system given by Eq. (1) describes how the recovery voltage y_1 is induced by the activation potential x_1. That is, $\dot{y}_1+\beta y_1=\beta\gamma x_1$. Motivated by this fact, in this study, we define a novel sliding mode (SM) to develop an adaptive SMC scheme that achieves the goals of state synchronization and anti-synchronization between two SFHN neuro-cell systems. The novel SM is defined such that the error of the activation potential converges to zero at a fixed time and remains on the sliding surface. Then, according to the second equation of Eq. (1), the error of the recovery voltage is also exponentially stabilized.

The novelty, features, and contributions of this study are summarized in the following.

(1) In contrast to previous works on SMC schemes,[28,36] a novel integral-type fixed-time stabilized sliding mode (IFSSM) is introduced. This IFSSM consists of the fractional-powered, proportional, and integral terms of two state variables. Furthermore, the two state variables are stabilized one by one. That is, on the sliding surface, one of the state variables becomes stable at a fixed time, then the other state variable is exponentially stabilized in sequence. The stability is proven by Theorem 1 in Sect. 3.

(2) To control the state synchronization and anti-synchronization between two SFHN neuro-cell circuits, the robust adaptive SMC scheme based on the novel IFSSM is performed on the basis of Theorem 2 in Sect. 3. The developed control scheme is divided into two parts. First, the error state trajectory is controlled to arrive at and remain on the sliding surface, which is defined by the IFSSM. Second, on the basis of the stable property of the IFSSM, the error of the activation potential first tends to zero at a fixed time, then remains on the sliding surface. The error of the recovery voltage is then exponentially stabilized.

(3) In previous studies, the problems of state synchronization and anti-synchronization were solved using different types of control method to complete control missions.[37–42] In contrast, in this work, the robust adaptive IFSSM control approach is introduced to simultaneously solve the control problems of state synchronization and anti-synchronization by suitably adjusting the design parameters, which are included in the control scheme.

(4) The developed adaptive IFSSM control approach, which contains four feedback gains, can dispose of the nonlinear dynamics without directly eliminating the nonlinear terms commonly adopted in the previous control approaches.[37–42] Meanwhile, the four gains are updated online using the proposed algorithm. We analyze the stability for both types of synchronization using Lyapunov stability theory.

(5) The validity and feasibility of the developed control scheme are verified by numerical simulation, demonstrating that the scheme can support most future implementations of neuronal circuits. In Sect. 4, numerical experiments are carried out to evaluate the performance of the proposed control approach.

The remainder of this paper contains the following. The control problems of state synchronization and anti-synchronization between two SFHN neuro-cell circuit systems are formulated in Sect. 2. In Sect. 3, the design procedures of the adaptive IFSSM control scheme are developed to achieve the two types of synchronization. In addition, proofs of the stability of the control systems are provided. Numerical simulations performed to verify the validity of the proposed control scheme are reported in Sect. 4. Finally, some concluding remarks are made in Sect. 5.

2. Control Problems of Synchronization

We consider the control problems of state synchronization and anti-synchronization between two SFHN neuro-cell systems with different ionic currents and EESs. The master SFHN neuro-cell system with a system uncertainty and an external disturbance is given the form in Eq. (1). The slave SFHN neuro-cell system has a similar form to Eq. (1) and is described as

$$\begin{cases} \dot{x}_2 = -x_2(x_2-1)(x_2-\alpha) - y_2 + I_{\text{ion}\_r} + I_r\cos(\omega_r t) + u(t) \\ \dot{y}_2 = \beta(\gamma x_2 - y_2) \end{cases}, \tag{3}$$

where x_2, y_2 are the state variables of the slave neuro-cell, I_{ion_r} is the ionic current in the slave neuro-cell, and $I_r\cos(\omega_r t)$ represents the ESS with amplitude Ir and frequency $f_r = \omega_r/2\pi$. In the control problems of the study, we take into account the different ionic currents and EESs of the SFHN neuro-cells in Eqs. (1) and (3), that is, $I_{ion\_r} \neq I_{ion\_m}$, $I_r \neq I_m$, $\omega_r \neq \omega_m$, and $u(t)$ is the control scheme to be designed. Furthermore, we assume that the master and slave neuro-cells in Eqs. (1) and (3), respectively, have unique solutions in the time interval $[t_0, \infty)$, $t_0 > 0$ for any given initial conditions. In addition, under the influences of the system uncertainty $\Delta(x_1,y_1)$, external disturbance $\delta(t)$, and control input $u(t)$, the two systems can still process bounded state trajectories. The control problems for state synchronization and anti-synchronization are formulated in the following.

The synchronous error states between the systems in Eqs. (1) and (3) are defined as

$$e_x(t) = x_2(t) - \lambda x_1(t), \quad e_y(t) = y_2(t) - \lambda y_1(t), \tag{4}$$

where $\lambda \in \{-1, 1\}$ is the scaling factor defining the relation between the synchronous systems. The control goal of the current problems is to design an appropriate control scheme $u(t)$ such that for any initial conditions of the two neuro-cells in Eqs. (1) and (3), the behavior of the response neuro-cell system converges to that of the master one, that is, $\lim_{t\to\infty} x_2(t) \to \lambda x_1(t)$, $\lim_{t\to\infty} y_2(t) \to \lambda y_1(t)$, where $\lambda = 1$ for state synchronization and $\lambda = -1$ for anti-synchronization.

For the case of $\lambda = 1$, by taking the derivative of Eq. (4) with respect to the normalized time t, the dynamics of the synchronous error states in the state synchronization are expressed as

$$\begin{cases} \dot{e}_x = [-f_1(x_1,x_2) + f_2(x_1,x_2)]e_x - \alpha e_x - e_y + (I_{ion\_r} - I_{ion\_m}) \\ \qquad + I_r \cos(\omega_r t) - I_m \cos(\omega_m t) - \Delta(x_1,y_1) - \delta(t) + u(t) \\ \dot{e}_y = \beta(\gamma e_x - e_y) \end{cases}, \tag{5}$$

where the functions $f_1(x_1,x_2) = x_1^2 + x_1x_2 + x_2^2$ and $f_2(x_1,x_2) = (\alpha+1)(x_1+x_2)$ are bounded because of the bounded state trajectories of $x_1(t)$, $x_2(t)$ for the master and slave neuron cell systems. $f_1(x_1,y_1)$ and $f_2(x_2,y_2)$ are, respectively, the state-dependent and time-varying coefficients of the synchronous error state $e_x(t)$.

For the case of anti-synchronization with $\lambda = -1$, by taking the derivative of Eq. (4) with respect to t, the dynamics of the synchronous error states are obtained as

$$\begin{cases} \dot{e}_x = [-f_3(x_1,x_2) - \alpha]e_x - e_y + f_4(x_1,x_2) + (I_{ion\_r} + I_{ion\_m}) \\ \qquad + I_r \cos(\omega_r t) + I_m \cos(\omega_m t) + \Delta(x_1,y_1) + d(t) + u(t) \\ \dot{e}_y = \beta(\gamma e_x - e_y) \end{cases}, \tag{6}$$

where the functions $f_3(x_1,x_2) = x_1^2 - x_1x_2 + x_2^2$ and $f_4(x_1,x_2) = (\alpha+1)(x_1^2+x_2^2)$ are bounded owing to the bounded state trajectories of $x_1(t)$, $x_2(t)$ for the master and slave neuro-cell systems. In this case, $f_4(x_1,x_2)$ in Eq. (6) is different from $f_2(x_1,x_2)$ in Eq. (5). $f_4(x_1, x_2)$ is regarded as a bounded external disturbance in the design of the control scheme.

Definition 1

The achievement of state synchronization or anti-synchronization between the two SFHN neuro-cells given by Eqs. (1) and (3) is equivalent to the state variables in Eqs. (5) and (6) tending to zero, that is, $\lim_{t\to\infty} e_x(t) \to 0$ and $\lim_{t\to\infty} e_y(t) \to 0$.

The state synchronization or anti-synchronization for the two neuro-cells given by Eqs. (1) and (3) is clearly equivalent to the stabilization of the synchronous error systems in Eqs. (5) or (6) by applying a suitable control scheme $u(t)$. The central goal of the current problem is to design a control $u(t)$ based on Definition 1. This $\lim_{t\to\infty} e_x(t) \to 0$ means that the behavior of the slave neuro-cell system given by Eq. (3) can synchronize or anti-synchronize that of the master one given by Eq. (1).

For the design of the control scheme for the state synchronization or anti-synchronization of two SFHN neuron cell systems, the effects of the nonlinear functions $f_i(x_1, x_2)$, $i = 1, 2, 3, 4$ are key points to be considered. Many approaches to compensating for nonlinear effects in chaotic control problems have been proposed, such as active control[37,38] and active SMC methods.[39-42] In this study, an IFSSM is proposed for the control, and a robust adaptive SMC with time-varying feedback gains is introduced to realize such control.

3. Design of Adaptive Control Scheme

In this section, an adaptive IFSSM control is proposed to achieve state synchronization or anti-synchronization between the neuro-cells given by Eqs. (1) and (3). The design approach of the adaptive IFSSM control scheme includes two basic steps. First, the IFSSM with the prescribed sliding motion is selected. The defined SM is designed such that on the sliding surface the synchronous error state $e_x(t)$ is first stabilized at a fixed time. Then, the synchronous error state $e_y(t)$ is exponentially stabilized to complete the synchronization. Second, adaptive control $u(t)$ is performed such that the state trajectory of $e_x(t)$, $e_y(t)$ in the phase plane arrives at and remains on the sliding surface despite the system uncertainties $\Delta(x_1,y_1)$ and the external disturbances $\delta(t)$.

Definition 2

The proposed IFSSM $s(t)$ is defined by

$$s(t) = [e_x(t)]^{p/q} + \frac{1}{\rho}\left[e_y(t) + \beta \int_{\tau=0}^{t} e_y(\tau) d\tau \right], \tag{7}$$

where $\rho > 0$, $p > 0$, $q > 0$ are odd integers with $1 < p/q < 2$ to escape the singularity of the equivalent control.

The novel IFSSM consists of the fractional-powered, proportional, and integral terms of two state variables. Theorem 1 ensures the fixed-time stability of $s(t) = 0$.

Theorem 1. For the IFSSM $s(t)$ defined in Eq. (7) with the second equation in Eq. (5) or (6), the fixed-time stability of $e_x(t)$ is guaranteed for $s(t)= 0$ associated with $\dot{s}(t) = 0$. First, $e_x(t) \to 0$ is achieved at a fixed time given by

$$T_s = \frac{\rho p}{\beta\gamma(p-q)}\left[e_x(t_0)\right]^{p/q-1} + t_0 . \tag{8}$$

Then, $e_x(t) = 0$ is maintained $\forall\, t \geq T_s > 0$, where $t = t_0 > 0$ is the time required for the state trajectory in the phase plane to arrive at $s(t) = 0$ from initial values $e_x(0)$, $e_y(0)$. Then, $e_y(t)$ is exponentially stabilized.

Proof

Assume that the system is controlled such that the state trajectory of $e_x(t)$, $e_y(t)$ arrives at $s(t) = 0$, then remains there, so that $\dot{s}(t) = 0$ is satisfied. By substituting the second equation in Eq. (5) or (6) into $\dot{s}(t) = 0$, we obtain the dynamical equation

$$\begin{aligned} &\dot{s}(t) = \frac{p}{q}\left[e_x(t)\right]^{p/q-1}\dot{e}_x(t) + \frac{1}{\rho}\left[\dot{e}_y(t) + \beta e_y(t)\right] = 0 \\ &\Rightarrow \frac{de_x(t)}{dt} + \frac{\beta\gamma q}{\rho p}\left[e_x(t)\right]^{2-p/q} = 0 \end{aligned} . \tag{9}$$

Integrating with respect to the normalized time $t \in [t_0, t]$, where $t_0 > 0$ is the time required for the state trajectory of $e_x(t)$, $e_y(t)$ in the phase plane to arrive at $s(t) = 0$ from the initial values $e_x(0)$, $e_y(0)$, yields

$$[e_x(t_0)]^{p/q-1} - [e_x(t)]^{p/q-1} = \frac{\beta\gamma(p-q)}{\rho p}(t - t_0). \tag{10}$$

The fixed time T_s taken to move from $e_x(t_0) \neq 0$ to $e_x(T_s) = 0$ is obtained as

$$T_s = \frac{\rho p}{\beta\gamma(p-q)}[e_x(t_0)]^{p/q-1} + t_0.$$

For $\beta > 0$ and $e_x(t) = 0, \forall t \geq T_s$ in the second equation of Eq. (5) or (6), it is clear that the stability of $e_y(t)$ on $s(t) = 0$ with $\dot{s}(t) = 0$ is guaranteed. That is,

$$\dot{e}_y(t) + \beta e_y(t) = 0 \Rightarrow e_y(t) = e_y(T_s)\exp(-\beta t), \ \forall t \geq T_s, \tag{11}$$

thus proving Theorem 1.

In the following, the robust and adaptive IFSSM control $u(t)$ in Eq. (5) or (6) for state synchronization or anti-synchronization is provided in Theorem 2. In the literature,[37,39,40] the developed control methods only solved a defined nonlinear chaotic control problem. In contrast, the proposed control scheme can be applied to solve both types of synchronization problem by simply suitably tuning the designed parameters.

Theorem 2. The adaptive IFSSM control scheme $u(t) = u_{eq}(t) + u_{sw}(t)$ in Eq. (5) or (6) is designed in the form

$$\begin{aligned} u_{eq}(t) &= -\frac{\beta\gamma q}{\rho p}[e_x(t)]^{2-p/q}, \\ u_{sw}(t) &= -\left[K_0(t) + K_1(t)|e_x(t)| + K_2(t)|e_y(t)| + K_3|s(t)|^n\right]\cdot \text{sign}(s(t)), \end{aligned} \tag{12}$$

where the designed parameters $\rho > 0$, $0 < n < 1$, $p > 0$, $q > 0$ are integers with $1 < p/q < 2$, $s(t)$ is the SM defined in Eq. (7), and sign(•) expresses the sign function. The adaptive feedback gains $K_i(t)$, $i = 0,1,2,3$ are updated online in accordance with the adaption algorithms

$$\begin{aligned} \dot{K}_0(t) &= \mu_0|e_x(t)|^{(p/q)-1}|s(t)|, \quad K_o(0) = 0, \quad \mu_0 > 0, \\ \dot{K}_1(t) &= \mu_1|e_x(t)|^{p/q}|s(t)|, \quad K_1(0) = 0, \quad \mu_1 > 0, \\ \dot{K}_2(t) &= \mu_2|e_x(t)|^{(p/q)-1}|e_y(t)||s(t)|, \quad K_2(0) = 0, \quad \mu_2 > 0, \\ \dot{K}_3(t) &= \mu_3|e_x(t)|^{(p/q)-1}|s(t)|^{n+1}, \quad K_3(0) = 0, \quad \mu_3 > 0. \end{aligned} \tag{13}$$

Then, $e_x(t)$, $e_y(t)$ in Eq. (5) or (6) approaches $s(t) = 0$ asymptotically and remains there, i.e., $\dot{s}(t) = 0$. This causes $e_x(t)$ to first converge to zero at a fixed time T_s approximated by Eq. (8). Then, $e_y(t)$ is exponentially stabilized in sequence. Thus, the state synchronization or anti-synchronization of the SFHN neuro-cells given by Eqs. (1) and (3) is accomplished.

Proof

(1) For the case of state synchronization, $\lambda = 1$, the candidate positive Lyapunov function for the dynamical system given by Eq. (5) is chosen as

$$V_1(t) = \frac{1}{2}s^2(t) + \sum_{i=0}^{3}\frac{p}{2q\mu_i}(K_i(t) - k_i)^2 \geq 0\,, \tag{14}$$

where $k_i > 0$, $i = 0, 1, 2, 3$ are positive constants satisfying

$$\begin{aligned} &k_0 > I_{\text{ion}\_r} + I_{\text{ion}\_m} + I_r + I_m + D_1 + D_2, \\ &k_1 > \left|f_1(x_1, x_2)\right| + \left|f_2(x_1, x_2)\right| + \alpha, \\ &k_2 > 1,\ k_3 > 0. \end{aligned} \tag{15}$$

Taking the derivative of Eq. (14) with respect to t with the solutions of the synchronous error system in Eq. (5), the selected SM in Eq. (7), and the adaptive IFSSM control scheme in Eqs. (12) and (13) yields

$$\begin{aligned} \dot{V}_1(t) &= s\left(\frac{p}{q}\left[e_x\right]^{p/q-1}\dot{e}_x + \frac{\beta\gamma}{\rho}e_x\right) + \sum_{i=0}^{3}\frac{p}{q\mu_i}(K_i(t) - k_i)\dot{K}_i(t) \\ &= \frac{p}{q}\left[e_x\right]^{p/q-1} s\cdot\Big[[-f_1(x_1, x_2) + f_2(x_1, x_2) - \alpha]e_x - e_y + (I_{\text{ion}\_m} - I_{\text{ion}\_r}) \\ &\quad + I_r\cos(\omega_r t) - I_m\cos(\omega_m t) - \Delta(x_1, y_1) - \delta(t) \\ &\quad - \left(K_0(t) + K_1(t)\left|e_x\right| + K_2(t)\left|e_y\right| + K_3\left|s\right|^n\right)\cdot\text{sign}(s)\Big] \\ &\quad + \sum_{i=0}^{3}\frac{p}{q\mu_i}(K_i(t) - k_i)\dot{K}_i(t), \end{aligned} \tag{16}$$

$$\begin{aligned} \dot{V}_1(t) \leq \frac{p}{q}\left|e_x\right|^{p/q-1}\left|s\right|\cdot\Big[&-\left(k_0 - I_{\text{ion}\_r} - I_{\text{ion}\_m} - I_r - I_m - D_1 - D_2\right) \\ &-\left(k_1 - \left|f_1\right| - \left|f_1\right| - \alpha\right)\left|e_x\right| - \left(k_2 - 1\right)\left|e_y\right| - k_3\left|s\right|^n\Big] < 0. \end{aligned} \tag{17}$$

From Eq. (15), it is proved that $V_1(t)$ is a positive definite function, and from Eq. (17), it is proved that it is a decreasing function. Thus, the zero equilibriums ($s = 0$, $K_i(t) = k_i$, $i = 0, 1, 2, 3$) are globally asymptotically stable. Therefore, $e_x(t)$, $e_y(t)$ in Eq. (5) will asymptotically approach the

sliding surface $s(t) = 0$ with $\dot{s}(t) = 0$ and remain there. On this surface, $e_x(t)$ is stabilized at a fixed time T_s by suitably choosing odd integers $\rho > 0$, $p > 0$, $q > 0$ with $1 < p/q < 2$ in accordance with Eq. (8). Then, the exponential stabilization of $e_y(t)$ is guaranteed by Eq. (11), thus realizing the state synchronization between the systems given by Eqs. (1) and (3) and completing the proof.

(2) For the case of anti-synchronization, $\lambda = -1$, the positive Lyapunov function for the system in Eq. (6) is selected to have the form in Eq. (14),

$$V_2(t) = \frac{1}{2}s^2(t) + \sum_{i=0}^{3}\frac{p}{2q\mu_i}(K_i(t) - g_i)^2 \geq 0\,, \tag{18}$$

where $g_i > 0$, $i = 0, 1, 2, 3$ are positive constants satisfying

$$\begin{aligned} &g_0 > \left|f_4(x_1, x_2)\right| + I_{\text{ion}\_r} + I_{\text{ion}\_m} + I_r + I_m + D_1 + D_2, \\ &g_1 > \left|f_3(x_1, x_2)\right| + \alpha, \\ &g_2 > 1,\ g_3 > 0. \end{aligned} \tag{19}$$

The remainder of the proof is similar to that for state synchronization and is omitted.

4. Numerical Simulation Studies

The hardware implementation of neuronal circuits is a mature technology. Before the future practical realization of the developed control scheme, its validity and feasibility must be verified. An advantage of the following numerical experiments is that the performance of the overall SFHN neuro-cell control system can be evaluated by simulations, thus supporting the further implementation of neuronal circuits.

In this section, numerical simulations are carried out to verify the validity of the proposed adaptive IFSSM control scheme. The fourth-order Runge-Kutta method with a time step of 0.0001 and initial conditions $(x_1, y_1) = (-0.5, 0.75)$, $(x_2, y_2) = (1.0, 0.6)$ is applied. The system parameters of the neuron cell are $\alpha = 0.25$, $\beta = 0.02$, and $\gamma = 0.25$. The EESs of the master and slave SFHN neuro-cells are assumed to have different current amplitudes and frequencies, and the corresponding values are taken as $I_m = 0.055$, $\omega_m = 0.1$, $I_r = 0.06$, $\omega_r = 0.15$. The ionic currents of the two SFHN neuro-cells are selected to be $I_{ion\_m} = 0.1$ and $I_{ion\_r} = 0.082$. The system uncertainty and the external disturbance of the master neuro-cell system are assumed to be $\Delta(x_1,y_1) = 0.15\sin(x_1)\cos(y_1)$ and $d(t) = 0.15\sin(0.05\pi t)$, respectively. The numerical simulations are first performed with the master and slave neuro-cells running without control. Then, at $t = 320$, the control input of the slave neuro-cell system is implemented for state synchronization or anti-synchronization between the two neuro-cell systems.

For state synchronization, $\lambda = 1$, the positive design parameters of the proposed adaptive IFSSM control scheme in Eq. (5) described by Eqs. (12) and (13) are chosen as $p = 31$, $q = 19$, $\rho = 0.01$, $n = 1/8$, $\gamma_0 = 6.3$, $\gamma_1 = 0.5$, $\gamma_2 = 4.8$, and $\gamma_3 = 1.2$. Furthermore, to demonstrate the

effectiveness of the proposed adaptive IFSSM control scheme, the existing adaptive SMC scheme introduced in Ref. 27 is employed for comparison. For the synchronous error system in Eq. (5), adaptive control scheme #A in Ref. 28 is

$$\sigma(t) = e_x(t) + 45e_y(t), \tag{20}$$

$$u(t) = e_y(t) - \left[2 + K_x(t)\left|e_x(t)\right| + K_y(t)\left|e_y(t)\right| + 0.5\left|\sigma(t)\right|^{1/2}\right] \cdot \text{sign}(\sigma(t)), \tag{21}$$

where $K_x(t)$ and $K_y(t)$ are, respectively, the adaptive feedback gains updated using the following adaptive rules:

$$\dot{K}_x(t) = \left|e_x(t)\right|\left|\sigma(t)\right|, \quad K_x(0) = 0, \tag{22}$$

$$\dot{K}_y(t) = 5\left|e_y(t)\right|\left|\sigma(t)\right|, \quad K_y(0) = 0. \tag{23}$$

Remark 1

The controllers in Eqs. (12) and (21) provide discontinuous control. To reduce the phenomenon of chattering, the sign function in the control is modified as tanh(s/ε), where ε is a sufficiently small design constant. This modification is valid in all the numerical simulations.

Remark 2

Different from adaptive control scheme #A in Eq. (21), the synchronous error state $e_y(t)$ in Eq. (5) is compensated adaptively without directed elimination by utilizing the equivalent control part $u_{eq}(t)$ in Eq. (12).

Figure 3 shows that $e_x(t)$, $e_y(t)$, and $s(t)$ behave irregularly when the control input is turned off, and when the control is implemented at t = 320, $e_x(t)$, $e_y(t)$ converge to zero and the state

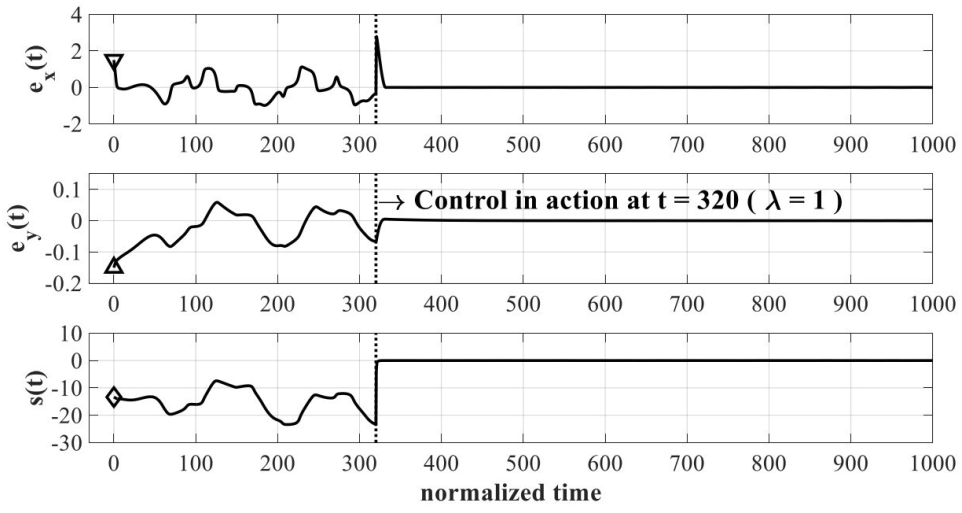

Fig. 3. Time responses of $e_x(t)$, $e_y(t)$, and $s(t)$ (λ = 1).

synchronization is completed. Figure 4 shows a comparison of the proposed adaptive IFSSM control scheme with adaptive control scheme #A in Ref. 28, which indicates that $e_x(t)$ is first stabilized at a fixed time. Then, $e_y(t)$ is exponentially stabilized for the adaptive IFSSM control scheme.

Figure 5 shows that the control input signals of both the proposed adaptive IFSSM control scheme and adaptive control scheme #A are continuous and chatter free. The peak value for the proposed control scheme is less than that for adaptive control scheme #A. The time responses of the adaptive feedback gains are shown in Fig. 6; the gains finally become constants. The figure indicates that $e_x(t)$, $e_y(t)$, and $s(t)$ all tend to zero in accordance with the adaption algorithm in Eq. (13).

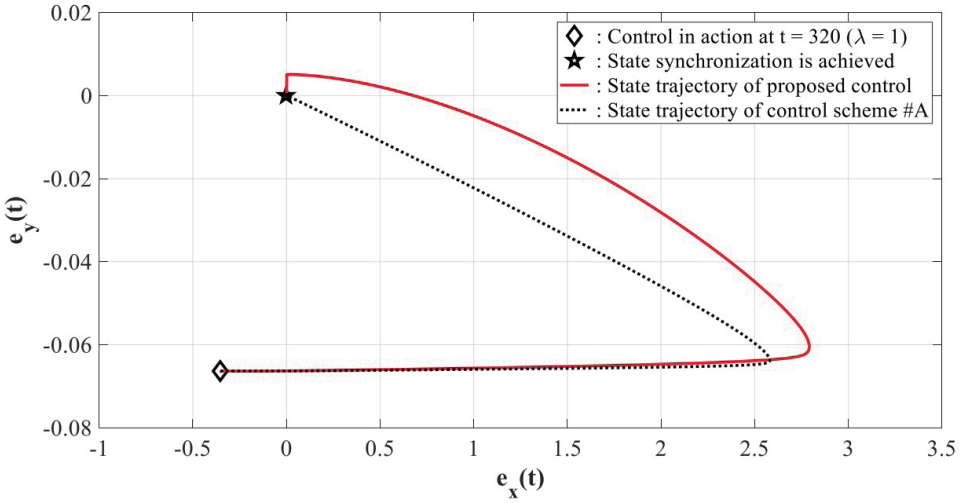

Fig. 4. (Color online) State trajectories of $e_x(t)$, $e_y(t)$ for the proposed control scheme and control scheme #A (λ = 1).

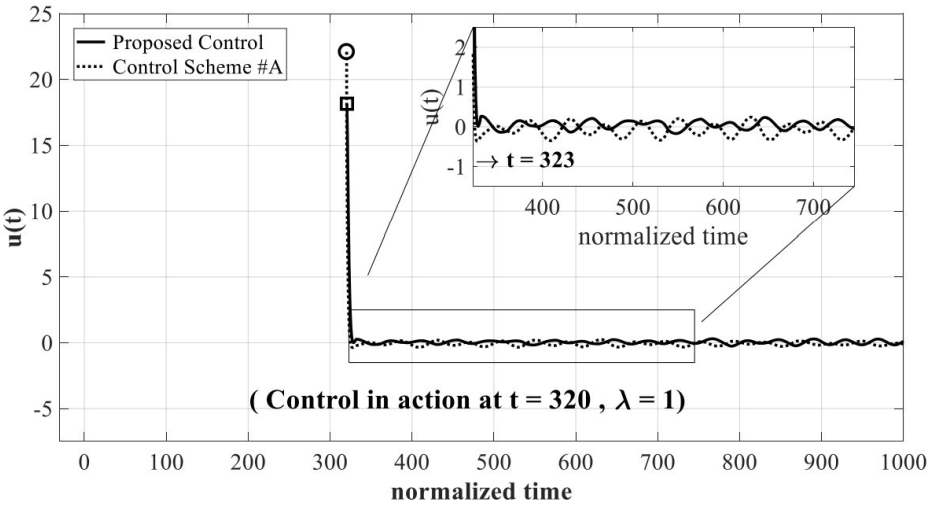

Fig. 5. Control signals of the proposed control scheme and control scheme #A (λ = 1).

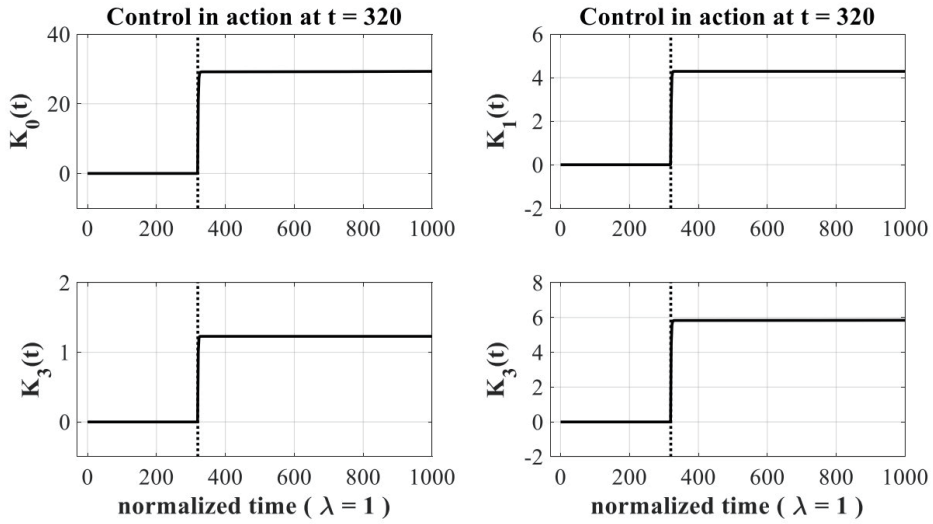

Fig. 6. Time responses of the adaptive feedback gains ($\lambda = 1$).

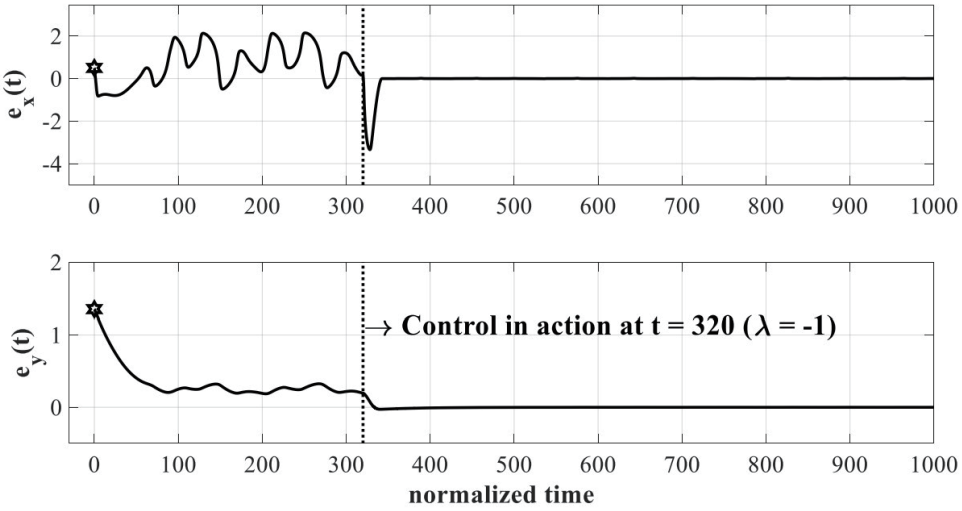

Fig. 7. Time responses of $e_x(t)$, $e_y(t)$ ($\lambda = -1$).

The case of state synchronization is achieved by the proposed control scheme in the aforementioned illustrated example. In the following, it is shown that the case of anti-synchronization is also achieved by the same control scheme with only suitable tuning of the designed parameters.

For the anti-synchronization, $\lambda = -1$, the positive design parameters of the proposed adaptive IFSSM control scheme of the system in Eq. (6) described by Eqs. (12) and (13) are taken as $p = 31$, $q = 19$, $\rho = 0.01$, $n = 1/8$, $\gamma_0 = 0.5$, $\gamma_1 = 0.005$, $\gamma_2 = 0.01$, and $\gamma_3 = 0.01$. Figures 7 and 8 show that anti-synchronization is achieved with stable characteristics similar to those in the case of state synchronization. That is, $ex(t)$ is first stabilized at a fixed time, then $e_y(t)$ is exponentially stabilized. Figure 9 illustrates the time responses of the state variables for the two SFHN neuro-

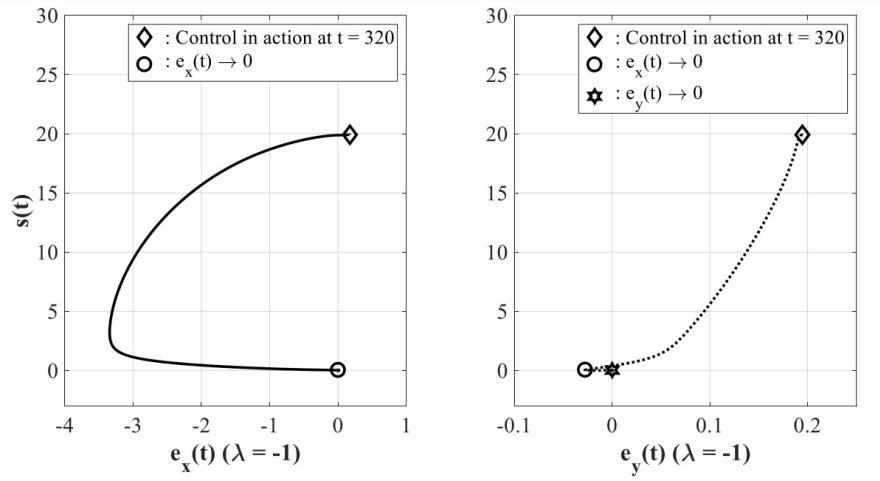

Fig. 8. State trajectories of $s(t)$ versus $e_x(t)$, $e_y(t)$ ($\lambda = -1$).

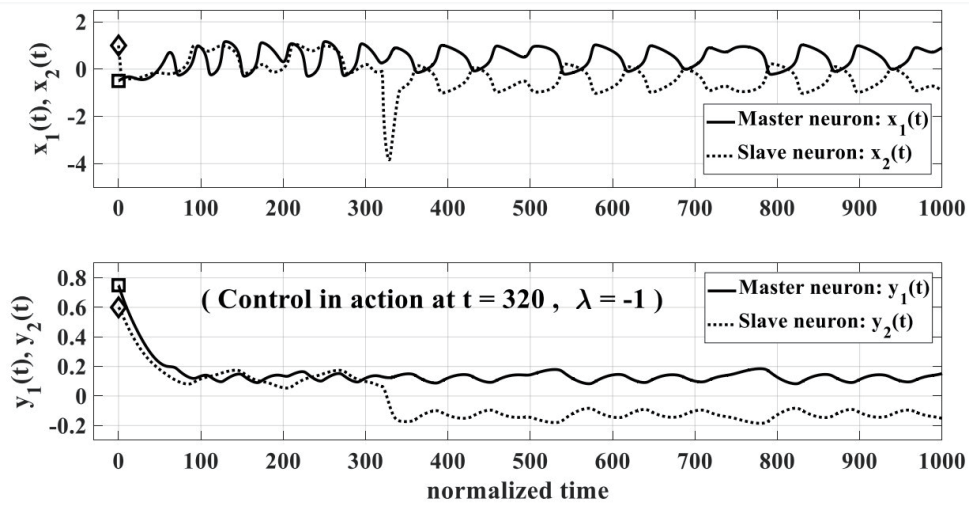

Fig. 9. Time responses of state variables for two anti-synchronized SFHN neuro-cells.

cells given by Eqs. (1) and (3). As expected, the state trajectories of the two neuro-cells separate from each other when different initial conditions are chosen. After the implementation of control at $t = 320$, both state variables become anti-synchronized, with the master neuro-cell system exhibiting system uncertainties and external disturbances.

5. Conclusions

We have proposed an adaptive IFSSM control scheme to solve the control problems of state synchronization and anti-synchronization between two SFHN neuro-cell systems in the presence of system uncertainty and external disturbance. For the control design, the novel defined IFSSM consists of the fractional-powered, proportional, and integral terms of two state

variables. The characteristics of the IFSSM on the sliding surface are also proven and experimentally verified. That is, the error state $e_x(t)$ is first stabilized at a fixed time, then the error state $e_y(t)$ is exponentially stabilized in sequence. The stability of both types of synchronization by applying the proposed adaptive IFSSM control scheme is proven in detail. Toward the future practical realization of neuronal circuits, numerical simulations are performed to verify the effectiveness of the present control scheme. It is also shown that the two control problems of state synchronization and anti-synchronization are solved by the proposed control scheme by simply suitably tuning the designed parameters.

Acknowledgments

We acknowledge the support from the School of Physics and Telecommunication Engineering, Yulin Normal University. This research was partly supported by the Scientific Research Fund Project (Grants G2020ZK15, G2020ZK16, and G2023ZK02) of Yulin Normal University.

References

1 L. Luo: Science **373** (2021) 6559. https://doi.org/10.1126/science.abg7285
2 K. Shaukat, S. Luo, V. Varadharajan, I. A. Hameed, S. Chen, D. Liu, and J. Li: Energies **13** (2020) 2509. https://doi.org/10.3390/en13102509
3 H. C. Tuckwell and J. Jost: Phys. A Statistical Mech. Appl. **388** (2009) 4115. https://doi.org/10.1016/j.physa.2009.06.029
4 B. Bao, A. Hu, H. Bao, Q. Xu, M. Chen, and H. Wu: Complexity **2018** (2018) 3872573. https://doi.org/10.1155/2018/3872573
5 D. Yang: Commun. Nonlinear Sci. Numer. Simulat. **18** (2013) 2783. https://doi.org/10.1016/j.cnsns.2013.02.004
6 M. M. Ibrahim and H. Jung: IEEE Access **7** (2019) 57894. https://doi.org/10.1109/ACCESS.2019.2913872
7 C. J. Thompson, D. C. Bardos, Y. S. Yang, and K. H. Joyner: Chaos Solit. Fract. **10** (1999) 1825. https://doi.org/10.1016/S0960-0779(98)00131-3
8 D. Q. Wei, X. S. Luo, B. Zhang, and Y. H. Qin: Nonlinear Anal. Real World Appl. **11** (2010) 1752. https://doi.org/10.1016/j.nonrwa.2009.03.029
9 Y. Gao: Chaos Solit. Fract. **21** (2004) 943. https://doi.org/10.1016/j.chaos.2003.12.033
10 A. Petrovas, S. Lisauskas, and A. Slepikas: Electron. Electr. Eng. **122** (2012) 117. https://doi.org/10.5755/j01.eee.122.6.1835
11 S. Binczak, S. Jacquir, J. M. Bilbault, V. B. Kazantsev, and V. I. Nekorkin: Neural Networks **19** (2005) 684. https://doi.org/10.1016/j.neunet.2005.07.011
12 Z. Liu, C. Wang, W. Jin, and J. Ma: Nonlinear Dyn. **97** (2019) 2661. https://doi.org/10.1007/s11071-019-05155-7
13 A. Tamaševicius, G. Mykolaitis, E. Tamaševiciute, and S. Bumeliene: Nonlinear Dyn. **81** (2015) 783. https://doi.org/10.1007/s11071-015-2028-y
14 J. Cosp, S. Binczak, J. Madrenas, and D. Fernandez: Inter. J. Electron. **101** (2014) 220. http://dx.doi.org/10.1080/00207217.2013.780263
15 Q. Xu and D. Zhu: IETE Tech. Rev. **38** (2021) 563. https://doi.org/10.1080/02564602.2020.1800526
16 D. Rajasekharan, A. Gaidhane, A. R. Trivedi, and Y. S. Chauhan: IEEE Trans. Computer-Aided Design Integ. Circuits Syst. **41** (2022) 2107. https://doi.org/10.1109/TCAD.2021.3101407
17 Y. Guo, C. Wang, Z. Yao, and Y. Xu: Phys. A **602** (2022) 127644. https://doi.org/10.1016/j.physa.2022.127644
18 Y. Guo, P. Zhou, Z. Yao, and J. Ma: Nonlinear Dyn. **105** (2021) 3603. https://doi.org/10.1007/s11071-021-06770-z
19 I. Hussain, S. Jafari, D. Ghosh, and M. Perc: Nonlinear Dyn. **104** (2021) 2711. https://doi.org/10.1007/s11071-021-06427-x
20 Y. Liu, W. J. Xu, J. Ma, F. Alzahrani, and A. Hobiny: Front Inform. Technol. Electron. Eng. **21** (2020) 1387. https://orcid.org/0000-0002-6127-000X

21 M. Ge, L Lu, Y. Xu, R. Mamatimin, Q. Pei, and Y. Jia: Chaos Solit. Fract. **133** (2020) 109645. https://doi.org/10.1016/j.chaos.2020.109645
22 G. Wang, Y. Xu, M. Ge, L. Lu, and Y. Jia: (AEÜ) Int. J. Electron. Commun. **120** (2020) 153209. https://doi.org/10.1016/j.aeue.2020.153209
23 Y. Zhang, Y. Xu, Z. Yao, and J. Ma: Nonlinear Dyn. **102** (2020) 1849. https://doi.org/10.1007/s11071-020-05991-y
24 C. Y. Yeh, J. Shiu, and H. T. Yau: Math. Prob. Eng. **2012** (2012) 745396. https://doi.org/10.1155/2012/745396
25 H. T. Yu and J. Wang: Acta Phys. Sin. **62** (2013) 170511. https://doi.org/10.7498/aps.62.170511
26 T. W. Lai, J. S. Lin, T. L. Liao, and J. J. Yan: Proc. 2007 Asian Simulation Conf. (AsiaSim, 2007) 142. https://doi.org/10.1007/978-3-540-77600-0_16
27 M. Rehan and K. S. Hong: Phys. Lett. A **375** (2011) 1666. https://doi.org/10.1016/j.physleta.2011.03.012
28 C. C. Yang and C. L. Lin: Nonlinear Dyn. **69** (2012) 2089. https://doi.org/10.1007/s11071-012-0410-6
29 C. Lu and X. Chen: J. Comp. Nonlinear Dyn. **11** (2016) 041011–1. https://doi.org/10.1115/1.4032074
30 Q. Zhang: Chaos Solit. Fract. **58** (2014) 22. http://dx.doi.org/10.1016/j.chaos.2013.11.002
31 D. Fan, X. Song, and F. Liao: Inter. J. Bifur. Chaos **28** (2018) 1850031. https://doi.org/10.1142/S0218127418500311
32 M. M. Ibrahim, M. A. Kamran, M. M. N. Mannan, I. H. Jung, and S. Kim: Sci. Rep. **11** (2021) 3884:1. https://doi.org/10.1038/s41598-021-82886-x
33 Y. Wang, F. Mina, Y. Cheng, and Y. Dou: Eur. Phys. J. Spec. Top. **230** (2021) 1751. https://doi.org/10.1140/epjs/s11734-021-00121-0
34 X. F. Zhang, J. Ma, Y. Xu, and G. D. Ren: Acta. Phys. Sin. **70** (2021) 090502. https://doi.org/10.7498/aps.70.20201953
35 Y. Zhang, C. Wang, J. Tang, J. Ma, and G. Ren: Science China Tech. Sci. **63** (2020) 2328. https://doi.org/10.1007/s11431-019-1547-5
36 Z. Zhao, X. Li, J. Zhang, and Y. Pei: Inter. J. Biomath. **10** (2017) 1750041. https://doi.org/10.1142/S1793524517500413
37 J. Wang, T. Zhang, and B. Deng: Chaos Solit. Fract. **31** (2007) 30. https://doi.org/10.1016/j.chaos.2005.09.006
38 Z. Wang and R. Guo: Symmetry **10** (2018) 552. https://doi.org/10.3390/sym10110552
39 W. Jawaada1, M. S. M. Noorani, and M. M. Al-sawalha: Chinese Phys. Lett. **29** (2012) 120505. https://doi.org/10.1088/0256-307X/29/12/120505
40 F. A. Khadra: J. Auto. Control **5** (2017) 1. https://doi.org/10.12691/automation-5-1-1
41 J. Guo, Y. Liu, and J. Zhao: J. Syst. Eng. Electro. **29** (2018) 571. https://doi.org/10.21629/JSEE.2018.03.14
42 S. Heidarzadeh and H. Salarieh: Iranian J. Sci. Tech. Trans. Mech. Eng. **43** (2019) 995. https://doi.org/10.1007/s40997-018-0209-2